Available online at www.sciencedirect.com
SCIENCE DIRECT®
Journal of Nuclear Materials 353 (2006) 119–126
journal of nuclear materials
www.elsevier.com/locate/jnucmat

Investigation of plutonium allotropic phase transformations through differential scanning calorimetry

T.G. Zocco *, D.S. Schwartz, J. Park

Los Alamos National Laboratory, Nuclear Materials Technology Division, MS G721, Los Alamos, NM 87545, USA

Received 1 December 2004; accepted 14 February 2006

Abstract

The investigation of phase transformations in high purity plutonium metal using a differential scanning calorimetry technique is reported, as a function of both heating and subsequent cooling. Data obtained in this study is compared to previous literature values, showing reasonable agreement for the various measurements. The unique features of this investigation are the very high purity metal used for experimentation, the isolation and analysis of the $\delta \leftrightarrow \delta'$ transformation, and the reverse transformation behavior of the five solid–solid allotropic transformations upon cooling. It is believed this is the first time complete cooling curves have been published for plutonium phase transformations. The results confirm the slow kinetics of transformations below the δ phase and the unusual martensitic-like behavior of the $\delta \rightarrow \gamma$ phase change.
Published by Elsevier B.V.

1. Introduction

Despite over 50 years of metallurgical research, the unusual behavior of Pu continues to be a source of new scientific discovery. Its mysterious behavior is believed to be caused by its complex electronic structure and the role f-electrons play in determining important characteristics such as crystalline structure. Its radioactive and toxic nature has limited the number of studies and experimental methods available to further understand the metallurgical behavior. Pure plutonium has six crystallographically different solid phases between room temperature and 640 °C (melting point). Existing as the complex monoclinic α phase at room temperature, the temperature must be raised to over ~320 °C (after three phase transformations: $\alpha \rightarrow \beta$, $\beta \rightarrow \gamma$ and $\gamma \rightarrow \delta$) for the metal to become cubic in symmetry. The crystal structures of the six allotropes of Pu are shown in Fig. 1, along with the approximate temperature range of stability. Interestingly, this cubic phase is the least dense, although having the most close-packed structure. The δ phase also has a negative coefficient of thermal expansion, further baffling investigators having the opportunity to investigate such an unusual material.

Previous examinations of the allotropic phase transformations of Pu have been studied using differential scanning calorimetry [1–5]. In each of these studies, data was collected and documented for all of the solid–solid allotropic phase transformations. In some cases the $\delta \rightarrow \delta'$ transformation was defined somewhat ambiguously or not observed at all [5],

* Corresponding author.
E-mail address: zocco@lanl.gov (T.G. Zocco).

0022-3115/$ - see front matter Published by Elsevier B.V.
doi:10.1016/j.jnucmat.2006.02.085

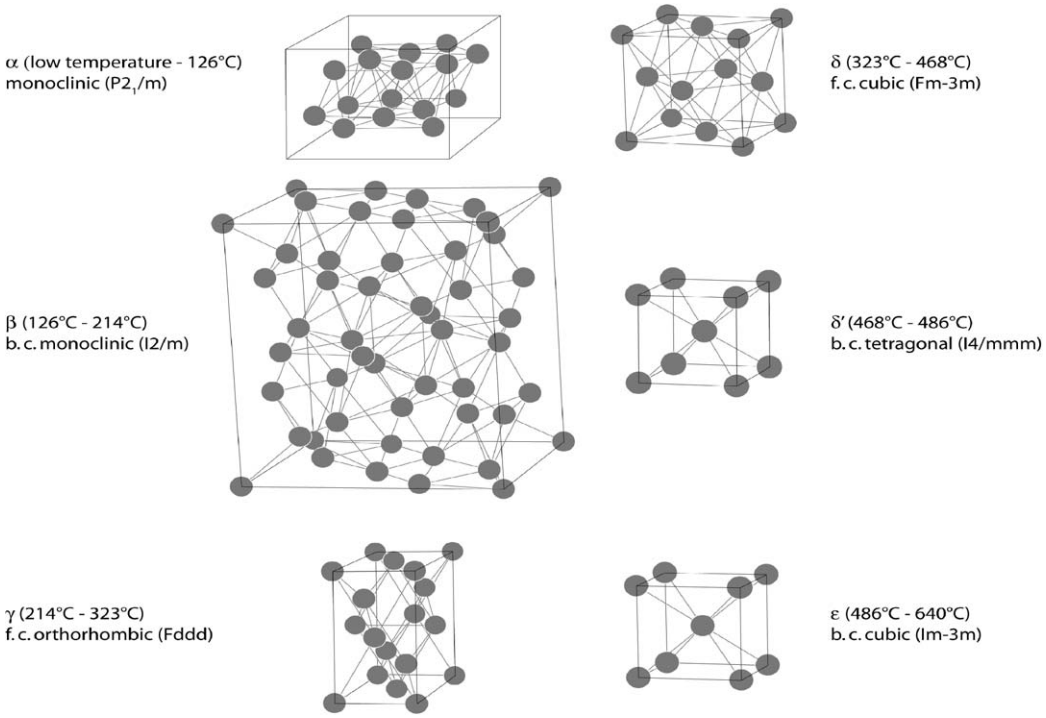

Fig. 1. The six allotropic crystal structures of Pu, labeled with their approximate temperature range of stability, Bravais lattice and space group. The unit cell sizes are roughly to scale.

probably due to relatively high impurity levels within the materials examined. For this study, high purity zone refined plutonium was used, allowing a clear definition of the $\delta \rightarrow \delta'$ and $\delta' \rightarrow \varepsilon$ transformation. Because of the purity of the plutonium, and improved DSC technology, it is also believed that the quantification of the plutonium phase transformation behavior is more accurate than previous investigations.

2. Experimental

The material used in this study was zone-refined, high purity plutonium [6]. The doubly electrorefined plutonium starting material with ~600 wppm total impurities was cast into rods. The material was then zone refined by passing a 10 mm wide 750 °C floating molten zone over the rod 10 consecutive times. Travel rates were 15 mm/h and the zone refining was performed under 10^{-5} Pa vacuum to eliminate any volatile impurities. This reduced the total impurity level of the metal to approximately 200 wppm, with the primary impurity being uranium (~100 wppm). The concentrations of impurities in the zone refined metal are shown in Appendix A.

To optimize heat flow to and from the samples while in the DSC instruments, thin disks of the material were fabricated using established procedures typically used to produce samples for transmission electron microscopy. The small flat disks (TEM foils) were typically 125–250 μm thick by 3.0 mm in diameter. For testing in the heat flux unit, samples weighed from 31 to 35 mg, while samples run in the power compensation unit weighed 15–25 mg (depending on the prepared thickness). Temperature ramp rates of 10 °C/min were used for both heating and cooling.

Two differential scanning calorimeters were used in this investigation, including a heat flux calorimeter (manufactured by Rheometrics Scientific) and a power compensation calorimeter (manufactured by Perkin–Elmer).[1] Identical material[2] was examined

[1] This study was not originally performed as a side-by-side comparison for purchase of the instruments, however, both units were available for use over the time of experimentation, hence a comparison was performed. It is believed that the calibration method used for the heat flux instrument is less accurate for measurement of heat release.

[2] Due to the radioactive isotopic decay of the material with time there was some difference in the chemistry between the samples run between instruments. The significance of these chemical changes has not been quantified and may be reflected in the results of this study.

Table 1
Experimental parameters

Instrument	Calorimeter type	Gas flow	Sample mass range (mg)	Heating/cooling rates (°C/min)
Rheometrics	Heat flux	Argon – 15 ml/min open Al pans	30–35	10/10
Perkin–Elmer	Power compensation	Argon – 20 ml/min crimped Al pans	15–25	10/10

in both instruments. Standard aluminum sample pans were used to improve response time for better accuracy and they also provided flat surfaces for excellent thermal contact with the thin and flat sample disks. Open pans (no lids) were used in the heat flux unit while crimped pans were used in the power compensation unit. In both cases, inert gas flow was used during the sample runs and typical parameters used for each instrument are shown in Table 1.

3. Results and discussion

3.1. Observations upon heating

Upon heating, transformations were clearly visible for each of the solid–solid phase transformations. In each case the peaks were well defined with significant peak intensities and each peak had a relatively symmetric shape. A representative set of endothermic peaks obtained upon heating is shown in Fig. 2, and a blow-up of the individual heat absorption peaks for each solid state transformation is shown in Fig. 3. Transformation temperatures and enthalpies measured on these instruments were in fairly good agreement between the two instruments, as seen in Table 2. The quality of this agreement is verified when compared to values measured by others as seen in Tables 3 and 4. Typically the transformation temperatures measured in this study differed by 1 °C or less.

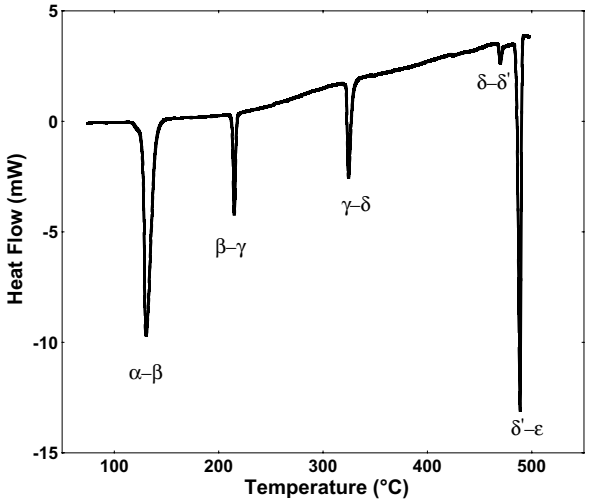

Fig. 2. Typical DSC heating scan with endothermic transformation peaks from each of the five solid–solid phase transformations in plutonium.

Although heat flux measurements using DSC are quite common, it is generally believed that power compensation provides better accuracy. Unfortunately, evidence from this study in comparison with others is not sufficient to conclusively prove this statement. Interestingly, whereas the transformation temperatures are in good agreement, the enthalpies appear to vary significantly. Some error is introduced by the analyst when measuring peak areas, but the variation in enthalpies seen in this investigation cannot be explained within this error. Also quite surprising is the fact that the larger the peak the greater the difference in the measured enthalpy (up to ~20%).

3.2. Observations upon cooling

Unlike previous investigations, this study also examined the transformation behavior upon cooling. As shown in Fig. 4, the $\varepsilon \rightarrow \delta'$ and the $\delta' \rightarrow \delta$ transformation peaks mirror their reverse transformations in both peak shape and onset temperature, with little undercooling. Comparison of the higher temperature transformation enthalpies shows a general agreement between the $\delta' \rightarrow \varepsilon/\varepsilon \rightarrow \delta'$ and the $\delta' \rightarrow \delta/\delta \rightarrow \delta'$ transformations suggesting complete transformations and little change to the specimen (such as oxidation) from high-temperature exposure. The shapes of the heat absorption curves on heating and heat release curves on cooling are quite similar for these two transformations, and the transformation onset temperatures display a normal amount of supercooling.

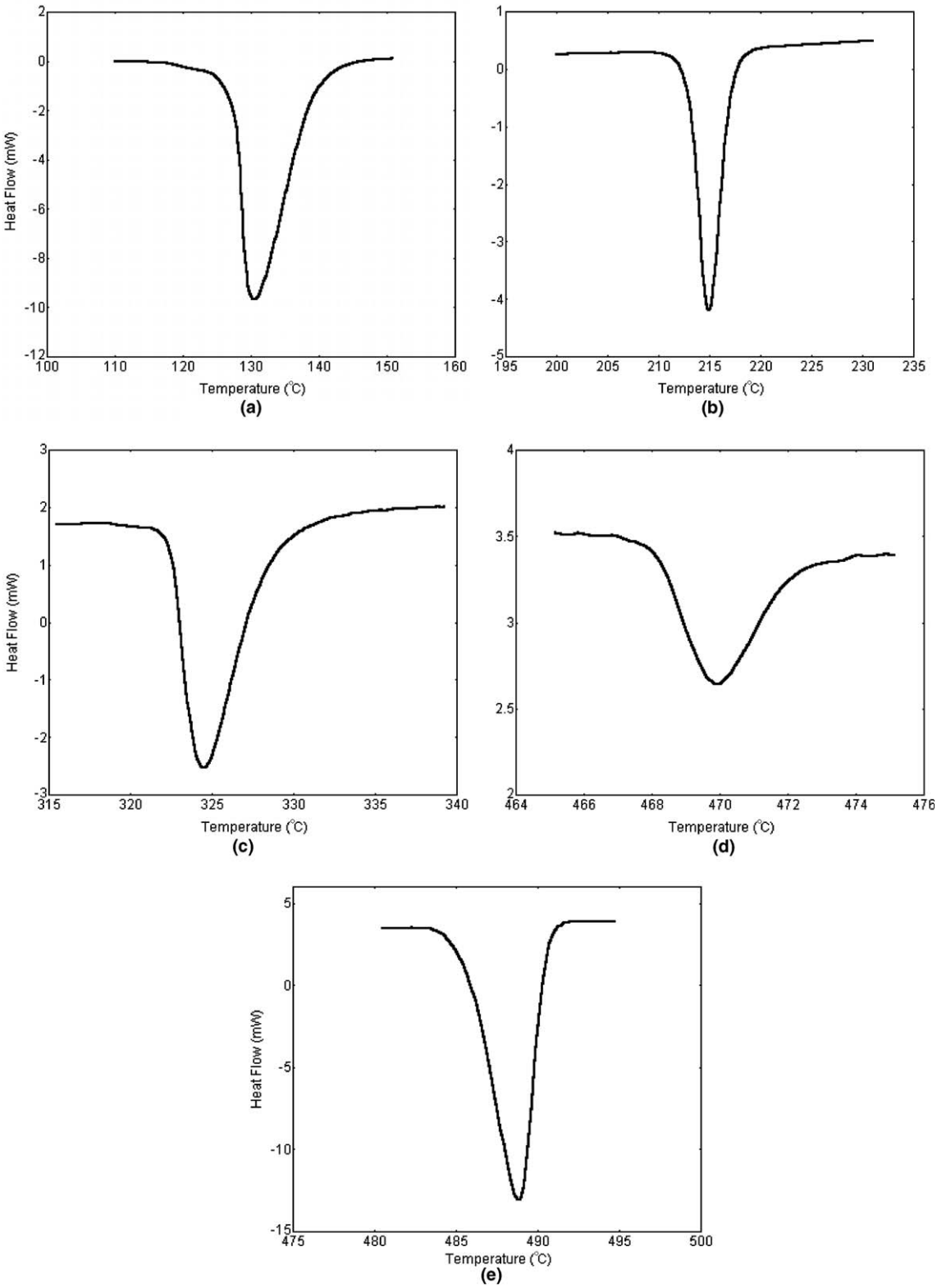

Fig. 3. Transformation peaks upon heating for the (a) $\alpha \rightarrow \beta$, (b) $\beta \rightarrow \gamma$, (c) $\gamma \rightarrow \delta$, (d) $\delta \rightarrow \delta'$, and (e) $\delta' \rightarrow \varepsilon$ phase transformations. Note significant changes in axis scales for each peak shown.

Table 2
Transformation temperatures and enthalpies from this work upon heating

Phase transformation	Onset temperature (°C) heat flux	Onset temperature (°C) power compensated	ΔT (°C) between instruments	ΔH (J/g) heat flux	ΔH (J/g) power compensated	Change in ΔH (J/g)
$\alpha \rightarrow \beta$	127.5 ± 0.3	126.25 ± 0.05	1.2	13.22 ± 0.29	15.43 ± 0.34	2.21
$\beta \rightarrow \gamma$	212.9 ± 0.3	213.90 ± 0.51	1.0	2.134 ± 0.05	2.18 ± 0.04	0.05
$\gamma \rightarrow \delta$	322.9 ± 1.6	323.42 ± 0.04	0.5	3.012 ± 0.18	2.35 ± 0.01	0.66
$\delta \rightarrow \delta'$	468.6 ± 2.3	467.60 ± 0.44	1.0	0.335 ± 0.03	0.273 ± 0.022	0.062
$\delta' \rightarrow \varepsilon$	485.6 ± 0.3	485.90 ± 0.13	0.3	9.205 ± 0.54	7.16 ± 0.16	2.04

Table 3
Transformation onset temperatures (T_o) from previous work

Phase transformation	T_o (°C) [2]	T_o (°C) [7]	T_o (°C) [4]	T_o (°C) [1]	Accepted T_o (°C) [7]
$\alpha \rightarrow \beta$	126.45	127	125		~115
$\beta \rightarrow \gamma$	216.55	215	215		~200
$\gamma \rightarrow \delta$	319.45	325	320		310
$\delta \rightarrow \delta'$	462.85	460	463	468 ± 2	452
$\delta' \rightarrow \varepsilon$	482.55	483	479	481	480

Table 4
Transformation enthalpies from previous work

Phase transformation	ΔH (J/g) [2]	ΔH (J/g) [5]	ΔH (J/g) [4]	ΔH (J/g) [3]
$\alpha \rightarrow \beta$	14.64 ± 0.58	16.02	15.50	15.49
$\beta \rightarrow \gamma$	2.033 ± 0.126	1.67	2.00	2.00
$\gamma \rightarrow \delta$	2.74 ± 0.13	2.97	2.98	2.98
$\delta \rightarrow \delta'$	0.43 ± 0.17	Peak not isolated	0.351	
$\delta' \rightarrow \varepsilon$	6.77 ± 0.78	7.70	7.00	

Upon further cooling the exothermic transformations are quite different from their endothermic allotropic counterparts found during heating. Phase transformation temperatures become substantially different and the peak intensities and shapes vary significantly. The reproducibility of these peaks is quite remarkable between runs. Fig. 6 shows an enlarged view of each of the transformation peaks found upon cooling. Note the unusual behavior in the $\delta \rightarrow \gamma$ phase transformation, long believed to be due to a martensitic-type phase change. The $\gamma \rightarrow \delta$ heating transformation (Fig. 3(c)) is a conventional solid–solid transformation, characterized by a single well-defined heat absorption spread over ~10 °C at the 10 °C/min scanning rate used in this study. However, the $\delta \rightarrow \gamma$ reversion on cooling (Fig. 6(c)) has a completely different character. First, it initiates at 260 °C (see Table 5), which is a supercooling of >60 °C below the heating transformation onset temperature. Secondly, the cooling transformation is characterized by a diminishing series of narrow heat release spikes, spread over

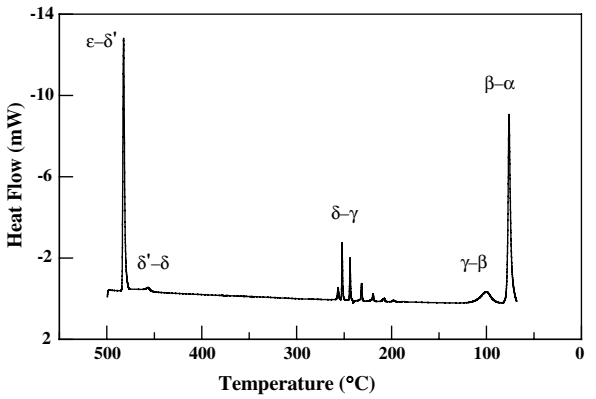

Fig. 4. Cooling curve from 500 °C to 60 °C showing the reverse transformations (note the reversal of the temperature axis). The sluggishness of the lower temperature phase transformations is readily apparent.

Table 5
Transformation temperatures and enthalpies from this work upon cooling

Phase transformation	Onset temperature (°C) heat flux	Onset temperature (°C) power compensated	ΔH (J/g) heat flux	ΔH (J/g) power compensated
$\varepsilon \rightarrow \delta'$	483.5 ± 0.1	483.9 ± 0.02	9.29 ± 0.46	7.12 ± 0.20
$\delta' \rightarrow \delta$	462.6 ± 1.3	461.2 ± 0.005	0.21 ± 0.04	0.21 ± 0.02
$\delta \rightarrow \gamma$	260.7 ± 0.8	257.1 ± 0.4[a]	[d]	2.14 ± 0.09[b]
$\gamma \rightarrow \beta$	[d]	113.6 ± 0.7	[d]	1.72 ± 0.013
$\beta \rightarrow \alpha$	80.4 ± 0.6	78.3 ± 0.5	8.91 ± 0.80	10.47 ± 0.46[c]

[a] Onset temperature of first peak in series (see text).
[b] Enthalpy change for all peaks in series summed together (see text).
[c] The DSC scan finished before this transformation was completed, therefore the enthalpy change is significantly underestimated.
[d] Not measured.

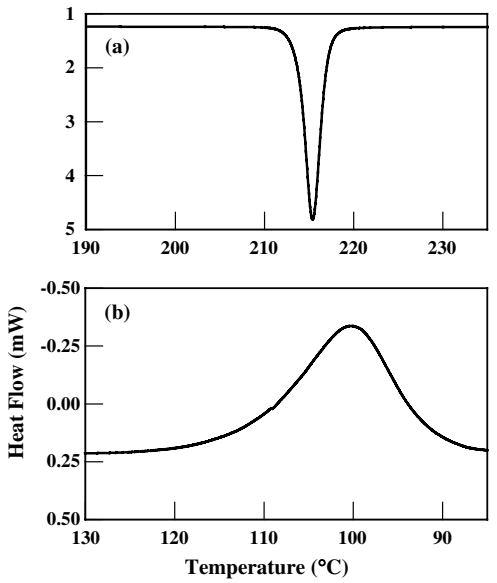

Fig. 5. A direct comparison of the (a) $\beta \rightarrow \gamma$ (heating) and (b) $\gamma \rightarrow \beta$ (cooling) transformations. Note that the temperature scales are both 45 °C long, whereas the heat flow scale is expanded by 4× in (b). The temperature axis is reversed in (b) so the transformation onsets are on the same side of the peak in both curves.

an 80 °C temperature range. This transformation was reported by Pascard [8] to occur primarily between 220 °C and 150 °C as measured by dilatometry; the significant difference between his measurements and ours may be due to the higher impurity levels of his material. Pascard also reported a smooth contraction of the δ starting at ~286 °C. However, we detected no evidence of any transformation above ~262 °C. If the total energy released over entire 260–180 °C temperature range is summed, it totals 2.14 ± 0.08 J/g, which is 10% less than the heat absorbed during the $\gamma \rightarrow \delta$ transformation. This evidence strongly suggests that while the $\gamma \rightarrow \delta$ transformation is conventional, the $\delta \rightarrow \gamma$ reversion is martensitic, i.e., strain controlled. The $\gamma \rightarrow \beta$ cooling transformation is also different in character than its heating counterpart. Fig. 5 directly compares the $\beta \rightarrow \gamma$ and $\gamma \rightarrow \beta$ transformations. The transformation onset temperature for the $\gamma \rightarrow \beta$ cooling transformation shows a ~100 °C supercooling relative to the $\beta \rightarrow \gamma$ heating transformation, an unusually large amount. The cooling transformation is much more sluggish, requiring 30 °C to complete as opposed to the 10 °C required for the heating transformation. In addition, the heat released is 27% less than the heat absorbed during the heating transformation, so it is likely that a significant amount of γ is retained below 113 °C.

4. Summary

This study provides information on the thermally-activated solid–solid phase transformation behavior of possibly the highest-purity plutonium metal yet examined. The material contained only 200 wppm total impurities with the majority (~100 wppm) comprised of uranium. The transformation behavior was analyzed using both heat flux and power compensated differential scanning calorimeters, resulting in relatively good agreement in the transformation onset temperatures and heats of transformation. Unlike some previous work, this investigation found clear evidence for the $\delta \rightarrow \delta'$ transformation, which could be definitively analyzed. The transformation behavior on cooling from the phase was examined in detail. The $\delta \rightarrow \gamma$ transformation was observed to occur at a significantly higher temperature than that reported by Pascard [8], but the same martensitic behavior was observed.

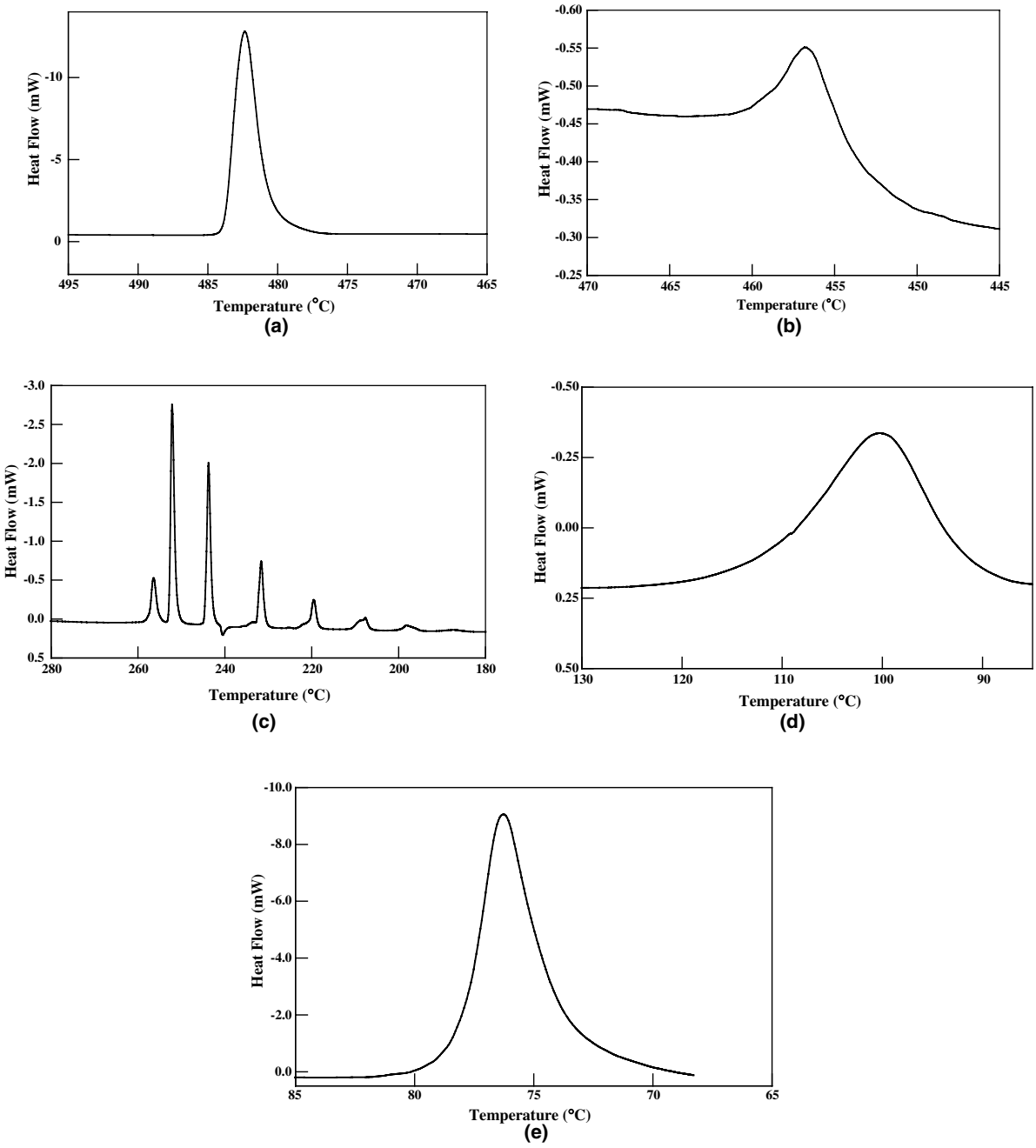

Fig. 6. Individual transformation peaks upon cooling for (a) $\varepsilon \rightarrow \delta'$, (b) $\delta' \rightarrow \delta$, (c) $\delta \rightarrow \gamma$, (d) $\gamma \rightarrow \beta$, and (e) $\beta \rightarrow \alpha$ (note the reversal of the temperature axis).

Anomalously large supercooling and slow transformation kinetics were seen for the $\gamma \rightarrow \beta$ cooling transformation. The high purity of the material used in this study adds confidence to the onset temperatures and transformation enthalpy values determined here. In addition to the analyzed data, heating and cooling curves have also been provided for future reference.

Appendix A

Table of impurities found in the zone refined metal examined

Impurity element	Concentration (ppm)	Minimum detection limit (MDL) (ppm)
Uranium	110.00	0.07
Potassium	40.00	14.00
Iron	<60.00	60.00
Tungsten	10.00	2.20
Sodium	<8.80	8.80
Phosphorus	7.00	5.60
Chromium	4.20	0.13
Tantalum	<2.20	2.20
Lead	1.70	0.08
Copper	0.80	0.13
Calcium	<0.50	0.50
Lithium	<0.40	0.40
Nickel	<0.40	0.40
Niobium	<0.40	0.04
Gold	<0.36	0.36
Germanium	<0.32	0.32
Rhenium	0.20	0.14
Hafnium	0.18	0.05
Beryllium	<0.18	0.18
Silver	<0.13	0.13
Rubidium	<0.11	0.11
Cobalt	<0.10	0.10
Cesium	<0.09	0.09
Manganese	<0.07	0.07
Palladium	<0.07	0.07
Indium	<0.06	0.06
Cadmium	0.05	0.04
Cerium	<0.04	0.04
Tin	<0.03	0.03
Total	174 ± 26	

References

[1] TH.K. Engel, Calorimetric Studies of δ, δ' and ε Plutonium, 23 (1967), p. 25.
[2] C.E. Rolon, G.F. Gallegos, J. Therm. Anal. 21 (1981) 159.
[3] F.L. Oetting, R.O. Adams, J. Chem. Thermodyn. 15 (1983) 537.
[4] J.W. Ward, P.D. Kleinschmidt, D.E. Peterson, in: A.J. Freeman, C. Keller (Eds.), Handbook on the Physics and Chemistry of the Actinides, Elsevier, Amsterdam, 1986, p. 309.
[5] E.M. Foltyn, J. Nucl. Mater. 172 (1990) 180.
[6] J.C. Lashley, M.S. Blau, K.P. Staudhammer, R.A. Pereyra, J. Nucl. Mater. 274 (1999) 315.
[7] O.J. Wick (Ed.), A Guide to the Technology, American Nuclear Society, 1980, p. 34.
[8] R. Pascard, in: E. Grison, W.B.H. Lord, R.D. Fowler (Eds.), Plutonium, Cleaver-Hume Press Ltd, 1960, p. 16.